International Journal of Automation and Computing 15(5), October 2018, 570-581
DOI: 10.1007/s11633-018-1134-y

An Energy-based Nonlinear Coupling Control for Offshore Ship-mounted Cranes

Yu-Zhe Qian[1,2] Yong-Chun Fang[1,2] Tong Yang[1,2]

[1] Institute of Robotics and Automatic Information System, Nankai University, Tianjin 300350, China

[2] Tianjin Key Laboratory of Intelligent Robotics, Nankai University, Tianjin 300350, China

Abstract: This paper proposes a novel nonlinear energy-based coupling control for an underactuated offshore ship-mounted crane, which guarantees both precise trolley positioning and payload swing suppressing performances under external sea wave disturbance. In addition to having such typical nonlinear underactuated property, as it is well known, an offshore ship-mounted crane also suffers from much unexpected persistent disturbances induced by sea waves or currents, which, essentially different from an overhead crane fixed on land, cause much difficulty in modeling and controller design. Inspired by the desire to achieve appropriate control performance against those challenging factors, in this paper, through carefully analyzing the inherent mechanism of the nonlinear dynamics, we first construct a new composite signal to enhance the coupling behavior of the trolley motion as well as the payload swing in the presence of ship′s roll motion disturbance. Based on which, an energy-based coupling control law is presented to achieve asymptotic stability of the crane control system′s equilibrium point. Without any linearization of the complex nonlinear dynamics, unlike traditional feedback controllers, the proposed control law takes a much simpler structure independent of the system parameters. To support the theoretical derivations and to further verify the actual control performance, Lyapunov-based mathematical analysis as well as numerical simulation/experimental results are carried out, which clarify the feasibility and superior performance of the proposed method over complicated disturbances.

Keywords: Energy-based control, offshore ship-mounted cranes, Lyapunov methods, underactuated, nonlinear control systems.

1 Introduction

Recently, a great surge in efforts have been seen to tackle the control problem of underactuated mechatronic systems, such as translational oscillator with rotational actuator (TORA) systems[1], underactuated vehicles[2, 3], underactuated surface vessels[4, 5], rotational-translational actuator (RTAC) systems[6], underactuated robotic systems[7], underactuated cranes[8–10], double-pendulum crane systems[11], etc.[12–19], which have less applicable control inputs than the to-be-controlled system degrees of freedom (DOFs). Being a typical underactuated nonlinear system, in marine industries, offshore cranes have been playing increasingly important roles as strong transportation tools primarily due to their merits of high transport capacity, super operation flexibility, less energy consumption, etc. Suffering from external disturbances such as sea waves, sea winds or currents, the ultimate regulation control objective of offshore ship-mounted crane systems is the accurate and efficient positioning of payloads with small swing against ship′s motion disturbances. However, during the transferring processes under harsh sea conditions, there is always unexpected payload swing induced by inertia and numerous external disturbances, which are dangerous and may cause severe impacts to the people or freights around. Hence, investigation of an effective control approach for an offshore ship-mounted crane is of significant importance in terms of both theoretical value and practical applications.

To effectively control an underactuated offshore ship-mounted crane, which contains a trolley moving along the boom and a payload connected by an inelastic wire, a preferred technique is to appropriately control the trolley motion by fully analyzing the inherent coupling mechanism between trolley movement, payload swing and ship′s motion. During past decades, many researches regarding offshore crane control approaches have been developed and reported in the literature, which can be roughly classified as linear methodology as well as nonlinear and intelligent strategies. For the former category, to simplify control design, the complex nonlinear crane model has been linearized around its equilibrium points, then a number of linear control approaches, such as linear quadratic regulator (LQR) control[20], optimal control[21], input shaping method[22], etc., can be utilized. However, as a means to achieve better control performance, the system nonlinearities cannot be neglected and should be strictly tackled, for which, nonlinear and intelligent

Research Article
Special Issue on Intelligent Control and Computing in Advanced Robotics
Manuscript received February 7, 2018; accepted May 3, 2018; published online July 10, 2018
Recommended by Associate Editor Yuan-Qing Xia

strategies, including anti-swing nonlinear controller[23], sliding-mode control[24], adaptive boundary controller[25], etc.[26], are proposed.

Additionally, although the mechanical structure of an offshore-mounted crane resembles that of a land-fixed overhead crane, which has the same characteristic of underactuation, the control problems for those systems are fairly different mainly due to the unmatched interference acting on the ship-mounted crane system induced by persistent sea wave disturbances, which, largely upgrade the difficulty in controller design for offshore ship-mounted cranes. Therefore, many ambitious control schemes proposed for land-fixed cranes covering double-pendulum cranes[11, 27–29], overhead cranes[8, 10, 30–32], tower cranes[9, 33], gantry cranes[34], etc., cannot be applied to offshore ship-mounted cranes directly. Moreover, to tackle the unmatched interference for a great variety of control systems, a number of methods like adaptive control algorithm[35], output tracking control[36], neural network-based control[37], are also investigated.

So far, it is still a quite open problem for offshore ship-mounted crane control due to some issues that remain unsolved, such as accurate positioning of payloads with lower swing in the marine environment. To this end, many attempts have been devoted to the improvement of high-performance control schemes for such systems. For example, besides the existing methods mentioned above[23–26], recently, two anti-swing nonlinear controllers considering ship roll disturbances for an offshore boom crane are proposed by Lu et al.[38], which contain a full state feedback controller as well as an output feedback controller. Moreover, in dealing with some unknown periodic sea wave disturbances, Qian et al.[39] design an efficient nonlinear adaptive learning control, which presents good robustness against everlasting disturbances and unknown parameters. For flexible marine installations, through analyzing the vessel dynamics, He et al.[40] develop a robust adaptive boundary control to achieve underwater positioning operations. By constructing an elaborate storage function, Sun et al.[41] provide a complete Lyapunov-based nonlinear anti-swing control method for an offshore crane, while for ship-mounted boom cranes with ship roll and heave movements, a nonlinear controller is proposed also by the same authors[42]. Moreover, for some systems with submerged payload hanging from offshore crane vessel, the nonlinear dynamic response has been investigated by Hannana and Bai[43], while a fuzzy sliding mode control approach has been proposed[44]. However, either linearized dynamic model or accurate knowledge is needed for the aforementioned control strategies, which are restrictive for the control issues of most offshore ship-mounted crane systems.

As a brief review, by examining the existing control approaches for offshore ship-mounted cranes, the following essential issues remain open and unresolved.

1) Most existing methods for complex offshore ship-mounted crane systems need to linearize the nonlinear crane dynamics or neglect some specific nonlinear terms around the equilibrium point, which may not obtain high control performance when the system states exceed the small ranges due to external disturbances, e.g., under harsh sea conditions.

2) For presently available closed-loop control methods for offshore cranes, they cannot theoretically guarantee the asymptotic stability of the equilibrium point, which is also a very important control problem for such underactuated systems. Moreover, since an offshore ship-mounted crane always suffers from some unmatched external disturbances, which are mainly caused by sea waves or currents, the accurate positioning of the payload with lower swing angle during transportation process is an imperative requirement for the control system in the industrial field.

3) Almost all existing control strategies are sensitive to external disturbances, which lack robustness for such offshore crane systems. Therefore, proposing of a high performance control law against undesired extraneous perturbations is of great importance.

Generally speaking, for control of mechanical systems, an energy-based controller designing approach is feasible and effective owing to its efficacy of energy elimination. In this regard, for instance, an energy-based control method for the regulation of overhead cranes is proposed by Sun and Fang[45], while an energy-based control of double pendulum cranes has also been developed[46].

Considering the previously mentioned facts, in this paper, we present a novel nonlinear energy-based coupling control for an offshore ship-mounted crane, which guarantees the asymptotic stability of the equilibrium point and achieves satisfactory control performance for various transportation tasks. Specifically, via introducing an elegant composite error signal, which enhances the inner coupling between system states and disturbed motion, an offshore ship-mounted crane system is then transformed into an interconnected system, which brings much convenience in controller design and stability analysis for the reconstructed crane model. Based on which, as is generally known that energy can reflect and describe the motion and status of a dynamical system, through choosing a proper Lyapunov candidate function, an energy-based controller is then designed. The convergence of the closed-loop system′s equilibrium point is proven by Lyapunov techniques and LaSalle′s invariance theorem. Finally, to illustrate the promising application prospect of the proposed control method, numerical simulation and experiments are both implemented, which clearly show its effectiveness as well as the robustness against external disturbances.

In summary, as the main contribution of this paper, the proposed method successfully achieves an improved control performance, which is presented as follows:

1) The newly defined coupling system states involve

the inherent mechanism of the nonlinear dynamics, which, along with the straightforward stability analysis, guarantees the superior control performance of the offshore ship-mounted crane system.

2) Unlike traditional energy-based control methods, the proposed controller takes full account of the state coupling of the nonlinear dynamics, which takes a much simpler structure independent of the system parameters.

3) The proposed controller is robust against numerous external disturbances, which is demonstrated by numerical/experimental results.

The remaining sections of the presentation are structured in the following manner. In Section 2, the original offshore crane dynamics is briefly introduced, and for the kernel part, a novel composite signal is developed and then the model transformation is implemented. Section 3 refers to the processing of controller design and stability analysis for the coupled crane system. Simulation results are given in Section 4, while experimental results are implemented in Section 5 to further demonstrate the superior performance of the proposed control scheme. Section 6 draws the main conclusion regarding this work.

2 Crane dynamics and model transformation

2.1 Dynamics and control objective

Considering the horizontal transportation stage of an offshore ship-mounted crane, see Fig. 1, the control issue can be depicted as precise positioning and swing elimination of payloads under external disturbances caused by sea waves or sea winds. Specifically, two frames are involved, which include the land-fixed frame I_n and the ship-fixed frame I_s. It can be seen from Fig. 1 that, in the inertia coordinate frame I_n, the axes y_n and z_n are vertical to the land and parallel with the ground, respectively; while in the non-inertia coordinate frame I_s, which is denoted as the ship frame, y_s and z_s axes are vertical to the shipboard and parallel with the ship deck, respectively.

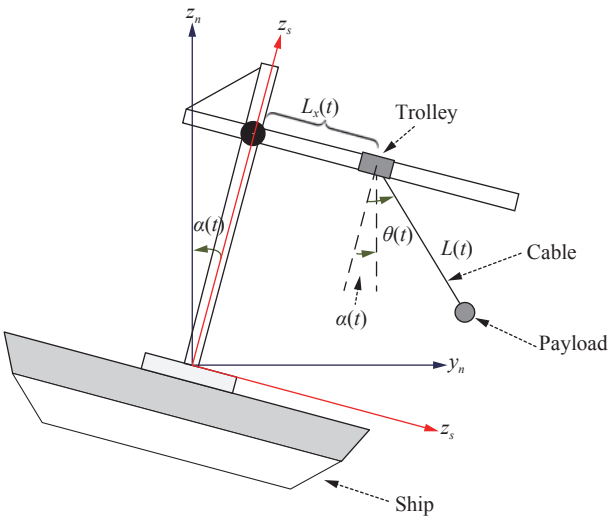

Fig. 1 Schematic illustration of an offshore ship-mounted crane

In our previous work, the dynamics of the 2-dimensional (2D) offshore ship-mounted crane, which contains the disturbing effect of ship's motion, can be given as follows[47]:

$$(m_1+m_2)\ddot{L}_x + m_2C_\theta L\ddot{\theta} - m_2LS_\theta\dot{\theta}^2 = F_x - f_{rx} + m_1gS_\alpha - m_2gS_\alpha - f_{L_x} \tag{1}$$

$$m_2LC_\theta\ddot{L}_x + m_2L^2\ddot{\theta} + m_2gLS_{\theta-\alpha} = -f_\theta \tag{2}$$

where m_1, m_2, L, g denote the trolley mass, the payload mass, the wire length and the gravitational constant, respectively. $L_x(t)$ and $\theta(t)$ represent the trolley position and the payload swing angle relative to the ship coordinate frame, respectively, which are also the to-be-controlled system states. $\alpha(t)$ is the ship's rolling angle relative to the land-fixed frame, which describes the external disturbance. In (1), $F(t)$ is the to-be-designed control input, and $f_{rx}(t)$ denotes the friction force between the trolley and the boom.

Besides, $f_{L_x}(t)$ and $f_\theta(t)$ are the disturbance-induced inertial forces acting on each sub-system with the following forms:

$$f_{L_x} = (m_1h + m_2h - m_2LC_\theta)\ddot{\alpha} + (m_1L_x + m_2L_x + m_2LS_\theta)\dot{\alpha}^2 + 2m_2L\dot{\theta}S_\theta\dot{\alpha} \tag{3}$$

$$f_\theta = m_2L(hC_\theta - L - L_xS_\theta)\ddot{\alpha} + m_2L(L_xC_\theta + hS_\theta)\dot{\alpha}^2 - 2m_2L\dot{L}_xS_\theta\dot{\alpha} \tag{4}$$

where h is a constant denoting the height of the boom.

In this paper, we mainly consider the transportation tasks from deck to deck, whose control objective is to position the payloads accurately with lower payload swing. Above all, before the controller design, the target position y_d can be described through analysing the geometric relationship as

$$y_d = L_{xd} + LS_{\theta_d} \tag{5}$$

where L_{xd} and θ_d are introduced as target values of the system states including trolley position and payload swing angle. Based on the fact that $\theta_d = \alpha(t)$, one has

$$L_{xd} = y_d - LS_\alpha \tag{6}$$

$$\theta_d = \alpha. \tag{7}$$

Then, the error signals $e_1(t)$ and $e_2(t)$ can be consequently defined as

$$e_1(t) = L_x - L_{xd} = L_x - y_d + LS_\alpha \tag{8}$$

$$e_2(t) = \theta - \theta_d = \theta - \alpha. \tag{9}$$

Hereto, the basic control tasks of an offshore ship-mounted crane can be summarized as follows:

1) To regulate the suspended payload from its initial position to the desired location, denoted as y_d in the land-fixed frame I_n, corresponding to the target values of system states $[L_{xd}, \theta_d]^{\mathrm{T}}$.

2) To suppress the residual payload swing (i.e., the swing after the cargo arrives at y_d) in the land-fixed frame I_n.

3) To eliminate the effect induced by external sea wave disturbances within finite time.

More specifically, to stabilize the offshore ship-mounted crane system at the desired equilibrium point, the main control objective is given by

$$[e_1(t)\ \ \dot{e}_1(t)\ \ e_2(t)\ \ \dot{e}_2(t)]^{\mathrm{T}} = [0\ \ 0\ \ 0\ \ 0]^{\mathrm{T}}. \tag{10}$$

From an arbitrary initial status in the presence of the unexpected additive disturbances f_{Lx}, f_θ. Namely that, a proper control law $F_x(t)$, which efficiently eliminates the oscillations of the platform and suppresses payload swing angle, is required to be proposed in this paper.

2.2 Model transformation

In order to enhance the coupling behavior of system states and facilitate the subsequent controller development and analysis, in this subsection, the model transformation is performed. Substituting formulas (3) and (4) into the original dynamics (1) and (2), respectively, and after some mathematical manipulations, one can obtain:

$$\begin{aligned}&(m_1+m_2)\left(\ddot{L}_x + h\ddot{\alpha}\right) + m_2C_\theta L\left(\ddot{\theta}-\ddot{\alpha}\right) - \\ &\quad m_2LS_\theta\left(\dot{\theta}-\dot{\alpha}\right)^2 = \\ &\quad F_x - f_{rx} + m_1gS_\alpha - m_2gS_\alpha - (m_1+m_2)L_x\dot{\alpha}^2\end{aligned} \tag{11}$$

$$\begin{aligned}&m_2LC_\theta\left(\ddot{L}_x + h\ddot{\alpha}\right) + m_2L^2\left(\ddot{\theta}-\ddot{\alpha}\right) + m_2gLS_{\theta-\alpha} = \\ &\quad m_2LS_\theta L_x\ddot{\alpha} - m_2L\left(L_xC_\theta + hS_\theta\right)\dot{\alpha}^2 + \\ &\quad 2m_2LS_\theta\dot{L}_x\dot{\alpha}.\end{aligned} \tag{12}$$

Herein, based on the form of (11) and (12), we define the novel composite error signals $\xi_1(t)$ and $\xi_2(t)$ as

$$\xi_1 = \dot{e}_1 + \lambda_\alpha\varphi(\alpha) + \lambda_\xi\phi(e_2) \tag{13}$$

$$\xi_2 = \dot{\theta} - \dot{\alpha} = \dot{e}_2 \tag{14}$$

where $\lambda_\alpha, \lambda_\xi \in \mathbf{R}^+$ are positive constant gains, $\varphi(\alpha)$, $\phi(e_2)$ denote the yet-to-construct scalar functions with regard to $\alpha(t)$ and $e_2(t)$.

Taking the time derivative of (13) and (14), respectively, we have

$$\dot{\xi}_1 = \ddot{e}_1 + \lambda_\alpha\dot{\varphi}(\alpha) + \lambda_\xi\frac{\partial\phi(e_2)}{\partial e_2}\xi_2 \tag{15}$$

$$\dot{\xi}_2 = \ddot{\theta} - \ddot{\alpha} = \ddot{e}_2 \tag{16}$$

while integrating those functions of (13) and (14), one obtains:

$$\begin{aligned}\int_0^t \xi_1(\tau)\,\mathrm{d}\tau = e_1 + \lambda_\alpha\int_0^t\varphi(\alpha(\tau))\,\mathrm{d}\tau + \\ \lambda_\xi\int_0^t\phi(e_2(\tau))\,\mathrm{d}\tau\end{aligned} \tag{17}$$

$$\int_0^t \xi_2(\tau)\,\mathrm{d}\tau = e_2. \tag{18}$$

Then, substituting (13)–(18) into (11) and (12), the coupled dynamics model can be rewritten as

$$\begin{aligned}&(m_1+m_2)\dot{\xi}_1 + m_2C_\theta L\dot{\xi}_2 - m_2LS_\theta\xi_2^2 = \\ &\quad F_x - f_{rx} + m_1gS_\alpha - m_2gS_\alpha - (m_1+m_2)L_x\dot{\alpha}^2 + \\ &\quad (m_1+m_2)(-\ddot{L}_{xd} - h\ddot{\alpha}) + \\ &\quad (m_1+m_2)(\lambda_\alpha\dot{\varphi}(\alpha) + \lambda_\xi\frac{\partial\phi(e_2)}{\partial e_2}\xi_2)\end{aligned} \tag{19}$$

$$\begin{aligned}&m_2LC_\theta\dot{\xi}_1 + m_2L^2\dot{\xi}_2 + m_2gLS_{\theta-\alpha} = \\ &\quad m_2L(S_\theta L_x\ddot{\alpha} - (L_xC_\theta + hS_\theta)\dot{\alpha}^2 + 2S_\theta\dot{L}_x\dot{\alpha}) + \\ &\quad m_2LC_\theta(-\ddot{L}_{xd} - h\ddot{\alpha}) + \lambda_\alpha m_2LC_\theta\dot{\varphi}(\alpha) + \\ &\quad \lambda_\xi m_2LC_\theta\frac{\partial\phi(e_2)}{\partial e_2}\xi_2.\end{aligned} \tag{20}$$

To facilitate the following analysis, based on (19) and (20), the matrix form of an offshore ship-mounted crane system is compacted as

$$\boldsymbol{M}_\xi\dot{\xi} + \boldsymbol{V}_\xi\xi = \boldsymbol{F}_c + \boldsymbol{f}_r + \boldsymbol{F}^* + \boldsymbol{F}_a \tag{21}$$

where the coupled system error vector is defined as

$$\xi(t) = \left[\ \xi_1(t)\quad \xi_2(t)\ \right]^{\mathrm{T}} \in \mathbf{R}^2 \tag{22}$$

the inertia matrix $\boldsymbol{M}_\xi(t) \in \mathbf{R}^{2\times2}$ and the centripetal Coriolis matrix $\boldsymbol{V}_\xi(t) \in \mathbf{R}^{2\times2}$ have the following forms as

$$\boldsymbol{M}_\xi = \begin{bmatrix} m_1+m_2 & m_2C_\theta L \\ m_2LC_\theta & m_2L^2 \end{bmatrix} \tag{23}$$

and

$$\boldsymbol{V}_\xi = \begin{bmatrix} 0 & -m_2LS_\theta\dot{\theta} \\ 0 & 0 \end{bmatrix}. \tag{24}$$

In (21), $\boldsymbol{F}_c \in \mathbf{R}^2$ denotes the control input as

$$\boldsymbol{F}_c = \left[\begin{array}{cc} F_x & 0 \end{array} \right]^{\mathrm{T}} \tag{25}$$

with F_x representing the only actuating force on trolley motion. The friction force vector $\boldsymbol{f}_r(t) \in \mathbf{R}^2$ is depicted as

$$\boldsymbol{f}_r = \left[\begin{array}{cc} -f_{rx} & 0 \end{array} \right]^{\mathrm{T}}. \tag{26}$$

In addition, for the coupling disturbance vectors, $\boldsymbol{F}^*(t) \in \mathbf{R}^2$ and $\boldsymbol{F}_a(t) \in \mathbf{R}^2$ are collected as

$$\boldsymbol{F}^* = \left[\begin{array}{cc} f_1^* & m_2 L f_2^* \end{array} \right]^{\mathrm{T}} \tag{27}$$

and

$$\boldsymbol{F}_a = \left[\begin{array}{cc} f_{a1} & f_{a2} \end{array} \right]^{\mathrm{T}} \tag{28}$$

respectively, the details are as follows:

$$f_1^* = m_1 g S_\alpha - m_2 g S_\alpha - (m_1 + m_2) L_x \dot{\alpha}^2 \tag{29}$$

$$\begin{aligned} f_2^* = {} & S_\theta L_x \ddot{\alpha} - (L_x C_\theta + h S_\theta) \dot{\alpha}^2 + 2 S_\theta \dot{L}_x \dot{\alpha} + \\ & m_2 L C_\theta (-\ddot{L}_{xd} - h\ddot{\alpha}) \end{aligned} \tag{30}$$

and

$$\begin{aligned} f_{a1} = {} & (m_1 + m_2)(-\ddot{L}_{xd} - h\ddot{\alpha}) + \\ & (m_1 + m_2)\left(\lambda_\alpha \dot{\varphi}(\alpha) + \lambda_\xi \frac{\partial \phi(e_2)}{\partial e_2} \xi_2\right) \end{aligned} \tag{31}$$

$$f_{a2} = \lambda_\alpha m_2 L C_\theta \dot{\varphi}(\alpha) + \lambda_\xi m_2 L C_\theta \frac{\partial \phi(e_2)}{\partial e_2} \xi_2. \tag{32}$$

Analogous to many other Euler-Lagrange systems[1–14], the following properties and assumption are also valid for the transformed model (21) as:

Property 1. The inertia matrix $\boldsymbol{M}_\xi$ in (23) is symmetric and positive definite.

Property 2. The matrix of $\left(\frac{1}{2}\dot{\boldsymbol{M}}_\xi - \boldsymbol{V}_\xi\right)$ presents skew symmetric property, namely that

$$x^{\mathrm{T}}\left(\frac{1}{2}\dot{\boldsymbol{M}}_\xi - \boldsymbol{V}_\xi\right) x = 0, \quad \forall x \in \mathbf{R}^2. \tag{33}$$

Assumption 1. Without loss of generality, considering the movement range of payload swing subject to the physical constraints, we assume that

$$-\frac{\pi}{2} \leq \theta - \alpha \leq \frac{\pi}{2}. \tag{34}$$

Remark 1. It is noteworthy that this assumption is widely used in the crane-related literature[6, 8, 11]. From an industrial perspective, considering that the payloads are heavy enough in practice and it is almost impossible to go above the trolley, this assumption is reasonable.

3 Controller design and stability analysis

In this section, a novel energy-based nonlinear coupling controller is derived on the basis of the coupled offshore ship-mounted crane model, which achieves simultaneous precise positioning and effective load swing suppression.

3.1 Controller design

First of all, instead of using feedforward or predictive control frameworks, we determine to derive an energy analysis-based controller. Based on this, for the control objective of (6), (7) and on the basis of the coupled error signal (22), the system mechanical energy is represented as follows:

$$E = \frac{1}{2}\xi^{\mathrm{T}} \boldsymbol{M} \xi + mgL(1 - C_{\theta-\alpha}) \tag{35}$$

whose time derivative can be calculated, by utilizing (21)–(32) and the property of (33), as

$$\dot{E} = \xi^{\mathrm{T}}(\boldsymbol{M}\dot{\xi} + \frac{1}{2}\dot{\boldsymbol{M}}\xi) + m_2 g L S_{\theta-\alpha}(\dot{\theta} - \dot{\alpha}) \tag{36}$$

which derives:

$$\begin{aligned} \dot{E} = {} & \xi_1 \left(F_x - f_{rx} + f_1^* + (m_1 + m_2)(-\ddot{L}_{xd} - h\ddot{\alpha}) + \right. \\ & \left. (m_1 + m_2)\lambda_\alpha \dot{\varphi}(\alpha) + (m_1 + m_2)\lambda_\xi \frac{\partial \phi(e_2)}{\partial e_2} \xi_2\right) + \\ & m_2 L \xi_2 (\lambda_\alpha C_\theta \dot{\varphi}(\alpha) + f_2^* + \lambda_\xi C_\theta \frac{\partial \phi(e_2)}{\partial e_2} \xi_2). \end{aligned} \tag{37}$$

Then, define the energy-based controller as

$$\begin{aligned} F_x = {} & -\lambda_\alpha (m_1 + m_2)\dot{\varphi}(\alpha) - \lambda_\xi (m_1 + m_2) \frac{\partial \phi(e_2)}{\partial e_2} \xi_2 - \\ & k_\xi \xi_1 - k_p \int_0^t \xi_1(\tau)\,\mathrm{d}\tau + f_{rx} - \\ & f_1^* + (m_1 + m_2)\left(\ddot{L}_{xd} + h\ddot{\alpha}\right) \end{aligned} \tag{38}$$

where $k_\xi, k_p \in \mathbf{R}^+$ are positive control gains.

Moreover, in order to decrease the closed-loop system energy, based on the form of (36), we choose

$$\lambda_\alpha C_\theta \dot{\varphi}(\alpha) = -f_2^* \tag{39}$$

and

$$\frac{\partial \phi(e_2)}{\partial e_2} = -1 \leq 0 \tag{40}$$

where the yet-to-construct functions defined in (13) can be consequently selected as

$$\varphi(\alpha) = -\frac{1}{\lambda_\alpha}\int_0^t \frac{f_2^*(\tau)}{C_\theta}\mathrm{d}\tau \tag{41}$$

and

$$\phi(e_2) = -(\theta - \alpha). \tag{42}$$

Substituting (41) and (42) into (38), the ultimate form of controller can be given as

$$\begin{aligned} F_x = &-k_\xi\xi_1 - k_p\int_0^t \xi_1(\tau)\,\mathrm{d}\tau + f_{rx} - \\ &f_1^* + (m_1+m_2)\left(\ddot{L}_{xd} + h\ddot{\alpha}\right) + \\ &(m_1+m_2)\frac{f_2^*}{C_\theta} + \lambda_\xi(m_1+m_2)\xi_2 \end{aligned} \tag{43}$$

where $k_\xi, k_p \in \mathbf{R}^+$ are positive control gains, with the coupling system states $\xi_1(t)$, $\xi_2(t)$ defined in (13) and (14), respectively.

3.2 Stability analysis

The stability of the overall closed-loop system is analyzed subsequently by using Lyapunov techniques and LaSalle's invariance theorem.

Theorem 1. Under the proposed nonlinear controller (43), the payload is driven to the desired position while the swing can be damped out globally in the sense that

$$\lim_{t\to\infty}\begin{bmatrix} e_1 & \dot{e}_1 & e_2 & \dot{e}_2 \end{bmatrix}^{\mathrm{T}} = \begin{bmatrix} 0 & 0 & 0 & 0 \end{bmatrix}^{\mathrm{T}}. \tag{44}$$

Proof. Let a positive definite Lyapunov candidate function $V(t)$, based on the energy of (35), be defined as

$$\begin{aligned} V = &\frac{1}{2}\xi^{\mathrm{T}}\boldsymbol{M}\xi + mgL(1 - C_{\theta-\alpha}) + \\ &\frac{1}{2}k_p\left(\int_0^t \xi_1(\tau)\,\mathrm{d}\tau\right)^2 \geq 0. \end{aligned} \tag{45}$$

Taking the time derivative of (45), and substituting the controller of (43) as well as the results of (36), (41) and (42), one leads to

$$\begin{aligned} \dot{V} = &\xi_1\left(-k_\xi\xi_1 - k_p\int_0^t \xi_1(\tau)\,\mathrm{d}\tau + k_p\int_0^t \xi_1(\tau)\,\mathrm{d}\tau\right) - \\ &\lambda_\xi m_2 L C_\theta \xi_2^2 \end{aligned} \tag{46}$$

implying that

$$\dot{V} = -k_\xi\xi_1^2 - \lambda_\xi m_2 L C_\theta \xi_2^2 \leq 0. \tag{47}$$

According to (47), it is easily shown that the closed-loop system states around the equilibrium points are stable in the Lyapunov sense, namely that

$$\xi_1(t), \xi_2(t) \in L_\infty \tag{48}$$

then, from (13) and (14), we have

$$\dot{L}_x(t), \dot{\theta}(t) \in L_\infty \tag{49}$$

which, together with (43) and (45), indicates

$$L_x(t), \int_0^t \xi_1(t)\,\mathrm{d}\tau, \int_0^t \xi_2(t)\,\mathrm{d}\tau \in L_\infty \tag{50}$$

as well as

$$e_1(t), e_2(t) \in L_\infty \Rightarrow \tag{51}$$

$$F_x(t) \in L_\infty. \tag{52}$$

Furthermore, to facilitate further analysis of the closed-loop system, let $\boldsymbol{\Lambda}$ be the largest invariant set in $\boldsymbol{S}$ as

$$\boldsymbol{S} = \left\{e_1, \dot{e}_1, e_2, \dot{e}_2 : \dot{V} = 0\right\} \tag{53}$$

in which, it follows from (47) and (53) that

$$\begin{aligned} &\xi_1 = 0,\ \xi_2 = 0 \Rightarrow \\ &\dot{\xi}_1 = 0,\ \dot{\xi}_2 = 0. \end{aligned} \tag{54}$$

Then, putting (54) into (21), by utilizing (8), (9) and (13)–(16), in the set $\boldsymbol{\Lambda}$, we have

$$\begin{aligned} &\dot{e}_2 = \xi_2 = 0 \\ &F_x - f_{rx} + f_{a1} + f_1^* = 0 \\ &f_{a2} + m_2 L f_2^* = 0 \\ &gS_{\theta-\alpha} = 0 \end{aligned} \tag{55}$$

implying that

$$\begin{aligned} &e_2 = \theta - \alpha = 0 \\ &\int_0^t \xi_1(\tau)\,\mathrm{d}\tau = 0 \Rightarrow \end{aligned} \tag{56}$$

$$e_1 = 0 \Rightarrow \tag{57}$$

$$\dot{e}_1 = \dot{L}_x - \dot{L}_{xd} = 0 \Rightarrow \tag{58}$$

$$L_x = L_{xd} \tag{59}$$

where it is not difficult to show that the largest invariant set $\boldsymbol{\Lambda}$ contains only the closed-loop system's equilibrium point:

$$\begin{bmatrix} e_1(t) & \dot{e}_1(t) & e_2(t) & \dot{e}_2(t) \end{bmatrix}^{\mathrm{T}} = \begin{bmatrix} 0 & 0 & 0 & 0 \end{bmatrix}^{\mathrm{T}}. \tag{60}$$

Finally, using LaSalle's invariant theorem, the conclusion of Theorem 1 can be obtained as

$$\lim_{t\to\infty}\begin{bmatrix} e_1 & \dot{e}_1 & e_2 & \dot{e}_2 \end{bmatrix}^{\mathrm{T}} = \begin{bmatrix} 0 & 0 & 0 & 0 \end{bmatrix}^{\mathrm{T}}. \quad (61)$$

□

Therefore, a direct application of LaSalle invariance theorem approves (44), which achieves the main control objective of accurate positioning of payload with lower swing angle under persistent external disturbances.

4 Numerical simulation

In this section, we implement some groups of numerical simulation tests in the environment of Matlab/Simulink and provide the simulation results to verify the performance of the designed offshore ship-mounted crane control system.

As stated previously, the control objective is to position the payload of the offshore ship-mounted crane to the expected accurate point against some external disturbances. Before the simulation/experiment, the dynamic model depicted in (21) is implemented in the Matlab/Simulink environment, and the parameters of the offshore ship-mounted crane system are chosen as

$$\begin{aligned} &m_1 = 4.3 \text{ kg},\ m_2 = 0.5 \text{ kg} \\ &L = 0.3 \text{ m},\ h = 0.58 \text{ m} \\ &g = 9.8 \text{ m/s}^2. \end{aligned}$$

4.1 Simulation 1

In this group of simulation, high control performance of the proposed controller (43) subjected to sea wave disturbances has been fully testified.

Firstly, the initial states of the system are selected as

$$L_x(0) = 0 \text{ m},\ \theta(0) = 0 \text{ deg}$$

and the desired position of payload and the ship motion disturbance are set as

$$\begin{aligned} &y_d = 0.15 \text{ m} \\ &\alpha = 0.5\cos(0.1t) - 0.5 \text{ deg}. \end{aligned}$$

To obtain proper performance, through carrying out abundant numerical simulations, the control gains for the proposed energy-based controller in this group are selected as follows:

$$\begin{aligned} &k_p = 8,\ k_\xi = 5 \\ &\lambda_\xi = 1.5,\ \lambda_\alpha = 5.5. \end{aligned}$$

Under unmatched sea wave disturbances, the following results of the designed ship-mounted crane control system are presented in Fig. 2, together with the results of the newly designed coupling states $\xi_1(t)$ and $\xi_2(t)$ in the last two subgraphs, so as to facilitate comparison.

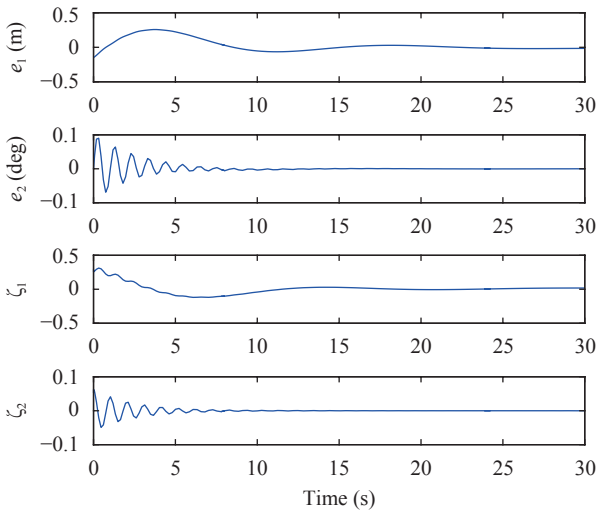

Fig. 2 Simulation 1: Trolley displacement error $e_1(t)$, payload swing angle $e_2(t)$, and the new composite signals $\xi_1(t)$ and $\xi_2(t)$, respectively.

It can be seen from these results that, the proposed controller achieves satisfactory performance under external disturbances, in the sense that the trolley position error $e_1(t)$ goes to zero within about 10 s while the swing angle error $e_2(t)$ is always bounded around the origin and can also converge to zero within 10 s during the entire transportation process.

Moreover, the new composite signals are also depicted in Fig. 2 to show more transient response of the offshore ship-mounted crane system, which greatly improves the efficiency of the control strategy with rapid convergence of system states.

4.2 Simulation 2

To further show the superiority of the proposed energy-based control method, in this group of simulation, some comparative numerical tests with linear quadratic regulator (LQR) controller are then implemented.

Generally speaking, a traditional LQR controller has the following form as[48]

$$F_x = -K_1 e_{Lx} - K_2 \dot{e}_{L_x} - K_3 e_\theta - K_4 \dot{e}_\theta$$

where to implement fair experiment, the proper control gains of LQR controller are solved by Matlab as follows:

$$\begin{aligned} &K_1 = 8.1,\ K_2 = 37.1 \\ &K_3 = -24.0,\ K_4 = 1.8. \end{aligned}$$

In this group of simulation, the desired position of payload and the ship motion disturbance are set as

$$y_d = 0.5 \text{ m}$$
$$\alpha = 0.18 \sin(0.1t) \text{ deg}$$

with the initial states both selected as

$$L_x(0) = 0 \text{ m}, \ \theta(0) = 0 \text{ deg}.$$

After careful tuning, to achieve fair simulations, the control gains for the proposed energy-based controller are selected as

$$k_p = 4.5, \ k_\xi = 2.5,$$
$$\lambda_\xi = 1, \ \lambda_\alpha = 5.$$

Corresponding simulation results are depicted in Fig. 3, which give the trolley position error $e_1(t)$, the payload swing angle $\theta(t)$ as well as the external disturbance $\alpha(t)$, respectively.

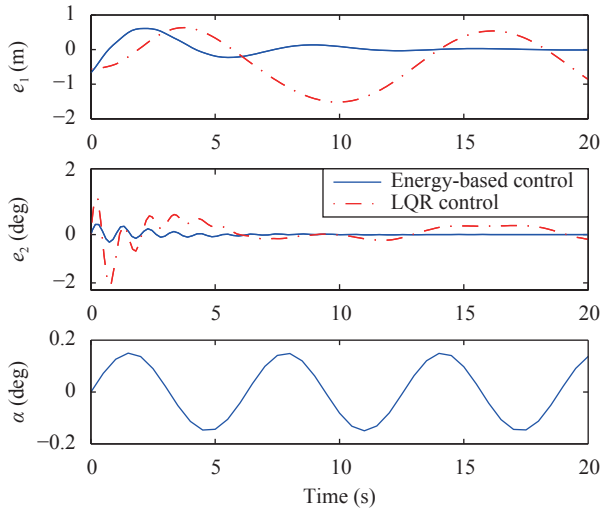

Fig. 3 Simulation 2: Trolley displacement error $e_1(t)$, payload swing angle $e_2(t)$ and ship roll disturbance $\alpha(t)$, respectively

It can be obviously seen from the comparative simulation results that, driven by the proposed controller, the error of trolley displacement and the payload swing angle both converge to zero within 10 s under persistent sea wave disturbances, which performs better than that of the LQR controller. Additionally, asymptotic convergence of system states can be guaranteed under the proposed controller, which shows a better performance than a simple linear controller such as LQR control.

5 Hardware experiment

From a practical perspective, this section exhibits some hardware experimental results to further test the performance of the proposed control method.

Based on a self-built offshore ship-mounted crane test bed[9, 39], some actual experiments are conducted to further verify the actual performance of the proposed approach. As shown in Fig. 4, this system consists of four parts, including a kernel control component, an actuating device, a mechanical framework and a chassis.

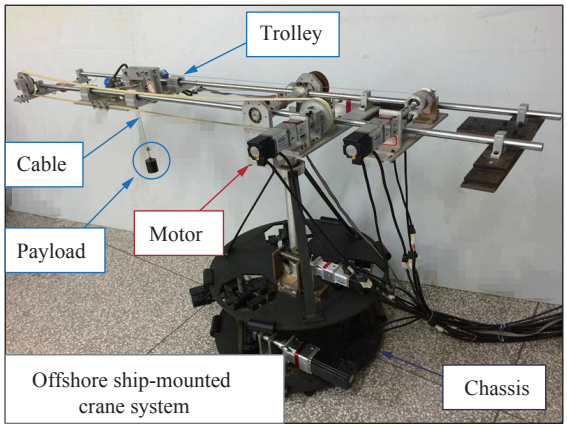

Fig. 4 Self-built offshore ship-mounted crane hardware experiment platform

In the system, the trolley moving along the boom and the steel rope connected with the suspending payload are driven by two SYNTRON alternating current (AC) servo motors, respectively. The swing angle of the payload is measured by angular sensors installed beneath the boom. Besides, the function of the chassis in this platform is to imitate the motion of sea waves and other unknown disturbances.

For real-time control algorithm implementation, Matlab/Simulink real-time Windows target running under Windows XP operating system is established for the control system. For the actuating device, seven actuators are communicated with seven AC servo motors so as to control the mechanical system. Moreover, one Google technology GT2-800-ACC2-V2.0V motion control board with I/O interfaces is employed as the data acquisition unit to collect data from the encoders and convey control signals to the driver so that the control voltage can be applied to the AC servo motors successfully.

Beforehand, regarding the utilized offshore ship-mounted crane hardware platform (see Fig. 4), the physical parameters of the testbed are configured as

$$m_1 = 3.5 \text{ kg}, \ m_2 = 0.5 \text{ kg}$$
$$L = 0.3 \text{ m}, \ h = 0.58 \text{ m}$$
$$g = 9.8 \text{ m/s}^2.$$

For sufficient verification, based on these conditions, we will carry out two groups of hardware experiments. Specifically, we will first demonstrate the satisfactory performance of the proposed control method under harsh sea wave disturbances. Then, in experiment Group 2, additional experiments will be implemented to verify the robustness against unexpected disturbances such as payload swing perturbations.

5.1 Experiment 1

In this subsection, the first group verifies the control performance of our approach under external sea wave disturbances, with the target value of payload set as

$$y_d = 0.15 \text{ m}$$

and the external disturbance chosen as

$$\alpha(t) = 0.3 \sin(\frac{\pi}{4}) \text{ deg}.$$

To obtain better performance, the control gains for the experiment are tuned as

$$k_p = 15,\ k_\xi = 25$$
$$\lambda_\xi = 10,\ \lambda_\alpha = 10.$$

As the control objective of this group of experiment is to drive the trolley to arrive at its target destination denoted as $y_d = 0.15$ m, while suppressing and eliminating the swing angle, Fig. 5 plots the experimental results of the system error signals. Under the action of the proposed energy-based control method, as clearly shown in Fig. 5, the trolley is successfully driven to reach the target position within a short time, and the payload swing angle is successfully suppressed within a small range of $[-0.3 \text{ deg}, 0.3 \text{ deg}]$.

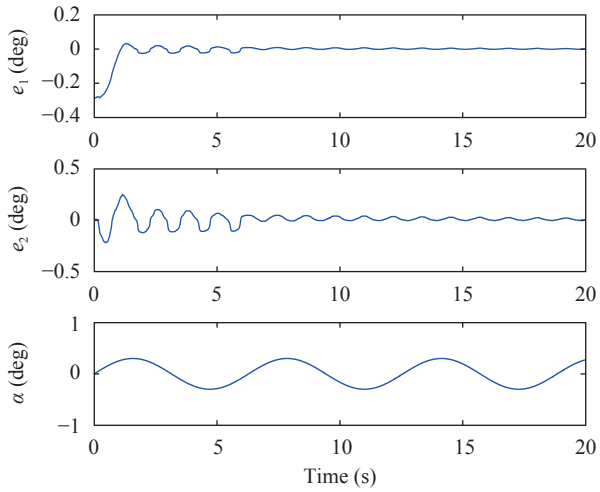

Fig. 5 Experiment 1: trolley displacement error $e_1(t)$, payload swing angle $e_2(t)$ and ship roll disturbance $\alpha(t)$, respectively

Besides, the ship roll disturbance $\alpha(t)$ is also depicted in the third subgraph of Fig. 5 to clearly show the imposed sustained external disturbances on an offshore ship-mounted crane.

Therefore, the accurate positioning and anti-swing performance of the proposed nonlinear controller can be fully demonstrated in this group of experiments.

5.2 Experiment 2

Furthermore, another test in this group is implemented to verify the robustness of the closed-loop control system against transient payload swing perturbation during transportation process, whose experimental results are shown in Fig. 6.

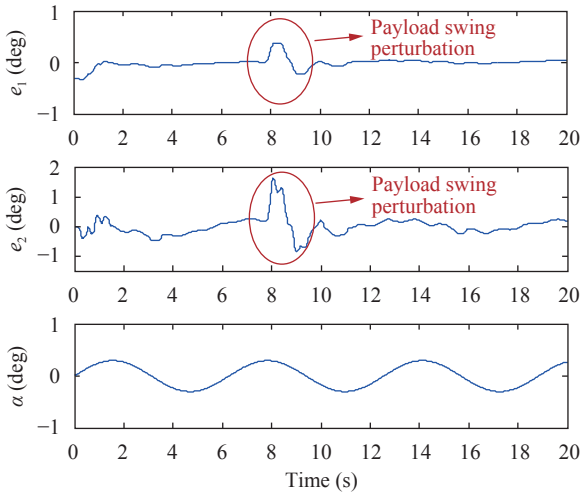

Fig. 6 Experiment 2: trolley displacement error $e_1(t)$, payload swing angle $e_2(t)$ and ship roll disturbance $\alpha(t)$, respectively, under transient payload swing perturbation

Specifically, for practical purposes, we set the target value of payload as

$$y_d = 0.5 \text{ m}$$

and choose the external disturbance as

$$\alpha(t) = 0.3 \sin(\frac{\pi}{4}) \text{ deg}.$$

Here, the control gains for the experiment are selected the same as in Experiment 1 as follows:

$$k_p = 15,\ k_\xi = 25$$
$$\lambda_\xi = 10,\ \lambda_\alpha = 10.$$

As clearly shown in Fig. 6, some unexpected external disturbances are added to the payload swing angles on purpose at about the 8th second (see the red marked places), while the control performance is still satisfactory in terms of asymptotic convergence, which demonstrates superior performance of the proposed controller.

Overall, with these simulation/experimental results, it can be concluded that the proposed energy-based control method allows for robustness, which is important for practical use.

6 Conclusions

This paper provides energy-based coupling control ap-

proach for an offshore ship-mounted crane. Successfully settling the challenges associated with underactuated property and unmatched external disturbances of such kind of systems, the proposed novel controller enhances the coupling behavior between trolley motion, payload swing and ship roll motion and then leads to an improved control performance. Based on the coupled model, a novel energy-based nonlinear controller is developed on the basis of system′s mechanical energy, then Lyapunov techniques as well as LaSalle′s invariant theorem are coherently utilized to further analyze the asymptotic stability of the closed-loop crane system. Simulation and experimental results are then included to demonstrate the superior control performance even in terms of transient payload swing perturbations. In forthcoming efforts, the control of 3D offshore ship-mounted crane which includes rotation motion of the boom should be taken into consideration, while more complex control problems such as tracking control are also involved in our future work.

Acknowledgements

This work was supported by National Natural Science Foundation of China (No. 11372144), National Science Fund for Distinguished Young Scholars of China (No. 61325017), and National Science Foundation of Tianjin.

References

[1] Y. M. Wu, N. Sun, Y. C. Fang, D. K. Liang. An increased nonlinear coupling motion controller for underactuated multi-TORA systems: Theoretical design and hardware experimentation. *IEEE Transactions on Systems, Man, and Cybernetics: Systems*, 2017, to be published. DOI: 10.1109/TSMC.2017.2723478.

[2] H. De Plinval, P. Morin, P. Mouyon. Stabilization of a class of underactuated vehicles with uncertain position measurements and application to visual servoing. *Automatica*, vol. 77, pp. 155–169, 2017. DOI: 10.1016/j.automatica.2016.11.012.

[3] H. Ashrafiuon, S. Nersesov, G. Clayton. Trajectory tracking control of planar underactuated vehicles. *IEEE Transactions on Automatic Control*, vol. 62, no. 4, pp. 1959–1965, 2017. DOI: 10.1109/TAC.2016.2584180.

[4] M. Mirzaei, N. Meskin, F. Abdollahi. Robust consensus of autonomous underactuated surface vessels. *IET Control Theory & Applications*, vol. 11, no. 4, pp. 486–494, 2017. DOI: 10.1049/iet-cta.2016.0930.

[5] B. S. Park, J. W. Kwon, H. Kim. Neural network-based output feedback control for reference tracking of underactuated surface vessels. *Automatica*, vol. 77, pp. 353–359, 2017. DOI: 10.1016/j.automatica.2016.11.024.

[6] N. Sun, Y. M. Wu, Y. C. Fang, H. Chen, B. Lu. Nonlinear continuous global stabilization control for underactuated RTAC systems: Design, analysis, and experimentation. *IEEE/ASME Transactions on Mechatronics*, vol. 22, no. 2, pp. 1104–1115, 2017. DOI: 10.1109/TMECH.2016.2631550.

[7] N. Sun, Y. M. Wu, Y. C. Fang, H. Chen. A new triple-stage stabilizing control method for two-wheeled inverted pendulum robots. In *Proceedings of IEEE International Conference on Real-time Computing and Robotics*, Angkor Wat, Cambodia, pp. 27–32, 2016. DOI: 10.1109/RCAR.2016.7783996.

[8] J. Smoczek, J. Szpytko. Particle swarm optimization-based multivariable generalized predictive control for an overhead crane. *IEEE/ASME Transactions on Mechatronics*, vol. 22, no. 1, pp. 258–268, 2017. DOI: 10.1109/TMECH.2016.2598606.

[9] N. Sun, Y. C. Fang, H. Chen, B. Lu, Y. M. Fu. Slew/translation positioning and swing suppression for 4DOF tower cranes with parametric uncertainties: Design and hardware experimentation. *IEEE Transactions on Industrial Electronics*, vol. 63, no. 10, pp. 6407–6418, 2016. DOI: 10.1109/TIE.2016.2587249.

[10] N. Sun, Y. C. Fang. Nonlinear tracking control of underactuated cranes with load transferring and lowering: Theory and experimentation. *Automatica*, vol. 50, no. 9, pp. 2350–2357, 2014. DOI: 10.1016/j.automatica.2014.07.023.

[11] N. Sun, Y. C. Fang, H. Chen, B. Lu. Amplitude-saturated nonlinear output feedback antiswing control for underactuated cranes with double-pendulum cargo dynamics. *IEEE Transactions on Industrial Electronics*, vol. 64, no. 3, pp. 2135–2146, 2017. DOI: 10.1109/TIE.2016.2623258.

[12] A. Roza, M. Maggiore, L. Scardovi. Local and distributed rendezvous of underactuated rigid bodies. *IEEE Transactions on Automatic Control*, vol. 62, no. 8, pp. 3835–3847, 2017. DOI: 10.1109/TAC.2017.2650562.

[13] N. Sun, Y. M. Wu, Y. C. Fang, H. Chen, B. Lu. Nonlinear continuous global stabilization control for underactuated RTAC systems: Design, analysis, and experimentation. *IEEE/ASME Transactions on Mechatronics*, vol. 22, no. 2, pp. 1104–1115, 2017. DOI: 10.1109/TMECH.2016.2631550.

[14] Z. B. Li, C. X. Zhou, Q. G. Zhu, R. Xiong. Humanoid balancing behavior featured by underactuated foot motion. *IEEE Transactions on Robotics*, vol. 33, no. 2, pp. 298–312, 2017. DOI: 10.1109/TRO.2016.2629489.

[15] S. Mahjoub, F. Mnif, N. Derbel. Second-order sliding mode approaches for the control of a class of underactuated systems. *International Journal of Automation and Computing*, vol. 12, no. 2, pp. 134–141, 2015. DOI: 10.1007/s11633-015-0880-3.

[16] A. H. D. Markazi, M. Maadani, S. H. Zabihifar, N. Doost-Mohammadi. Adaptive fuzzy sliding mode control of under-actuated nonlinear systems. *International Journal of Automation and Computing*, vol. 15, no. 3, pp. 364–376, 2018. DOI: 10.1007/s11633-017-1108-5.

[17] B. K. Sahu, B. Subudhi, M. M. Gupta. Stability analysis of an underactuated autonomous underwater vehicle using extended-Routh′s stability method. *International Journal of Automation and Computing*, vol. 15, no. 3, pp. 299–309, 2018. DOI: 10.1007/s11633-016-0992-4.

[18] M. Hashemi, J. Askari, J. Ghaisari, M. Kamali. Robust adaptive actuator failure compensation for a class of uncertain nonlinear systems. *International Journal of Automation and Computing*, vol. 14, no. 6, pp. 719–728, 2017. DOI: 10.1007/s11633-016-1016-0.

[19] W. Sun, W. X. Yuan, Y. Q. Wu. Adaptive tracking control of mobile manipulators with affine constraints and under-actuated joints. *International Journal of Automation*

and Computing, 2016, to be published. DOI: 10.1007/s11633-015-0934-6.

[20] R. M. T. R. Ismail, N. D. That, Q. Ha. Modelling and robust trajectory following for offshore container crane systems. *Automation in Construction*, vol. 59, pp. 179–187, 2015. DOI: 10.1016/j.autcon.2015.05.003.

[21] D. Kim, Y. Park. 3-Dimensional position control scheme for mobile harbor crane. In *Proceedings of the 15th International Conference on Control, Automation and Systems*, Busan, South Korea, pp. 2058–2061, 2015. DOI: 10.1109/ICCAS.2015.7364707.

[22] J. Huang, E. Maleki, W. Singhose. Dynamics and swing control of mobile boom cranes subject to wind disturbances. *IET Control Theory & Applications*, vol. 7, no. 9, pp. 1187–1195, 2013. DOI: 10.1049/iet-cta.2012.0957.

[23] Y. C. Fang, P. C. Wang, N. Sun, Y. C. Zhang. Dynamics analysis and nonlinear control of an offshore boom crane. *IEEE Transactions on Industrial Electronics*, vol. 61, no. 1, pp. 414–427, 2014. DOI: 10.1109/TIE.2013.2251731.

[24] Q. H. Ngo, K. S. Hong. Sliding-mode antisway control of an offshore container crane. *IEEE/ASME Transactions on Mechatronics*, vol. 17, no. 2, pp. 201–209, 2012. DOI: 10.1109/TMECH.2010.2093907.

[25] W. He, S. S. Ge, S. Zhang. Adaptive boundary control of a flexible marine installation system. *Automatica*, vol. 47, no. 12, pp. 2728–2734, 2011. DOI: 10.1016/j.automatica.2011.09.025.

[26] N. P. Nguyen, T. N. Phan, Q. H. Ngo. Autonomous offshore container crane system using a fuzzy-PD logic controller. In *Proceedings of the 16th International Conference on Control, Automation and Systems*, Gyeongju, South Korea, pp. 1093–1098, 2016. DOI: 10.1109/ICCAS.2016.7832447.

[27] N. Sun, Y. M. Wu, Y. C. Fang, H. Chen. Nonlinear antiswing control for crane systems with double-pendulum swing effects and uncertain parameters: Design and experiments. *IEEE Transactions on Automation Science and Engineering*, 2017, to be published. DOI: 10.1109/TASE.2017.2723539.

[28] N. Sun, Y. C. Fang, Y. M. Wu, H. Chen. Adaptive positioning and swing suppression control of underactuated cranes exhibiting double-pendulum dynamics: Theory and experimentation. In *Proceedings of Youth Academic Annual Conference of Chinese Association of Automation*, Wuhan, China, pp. 87–92, 2016. DOI: 10.1109/YAC.2016.7804870.

[29] N. Sun, Y. M. Wu, H. Chen, Y. C. Fang. An energy-optimal solution for transportation control of cranes with double pendulum dynamics: Design and experiments. *Mechanical Systems and Signal Processing*, vol. 102, pp. 87–101, 2018. DOI: 10.1016/j.ymssp.2017.09.027.

[30] B. Lu, Y. C. Fang, N. Sun. A new sliding-mode like nonlinear controller for overhead cranes with smooth control inputs. In *Proceedings of American Control Conference*, Boston, USA, pp. 252–257, 2016. DOI: 10.1109/ACC.2016.7524924.

[31] H. Chen, Y. C. Fang, N. Sun. A swing constraint guaranteed MPC algorithm for underactuated overhead cranes. *IEEE/ASME Transactions on Mechatronics*, vol. 21, no. 5, pp. 2543–2555, 2016. DOI: 10.1109/TMECH.2016.2558202.

[32] H. Chen, Y. C. Fang, N. Sun. Optimal trajectory planning and tracking control method for overhead cranes. *IET Control Theory & Applications*, vol. 10, no. 6, pp. 692–699, 2016. DOI: 10.1049/iet-cta.2015.0809.

[33] M. Böck, A. Kugi. Real-time nonlinear model predictive path-following control of a laboratory tower crane. *IEEE Transactions on Control Systems Technology*, vol. 22, no. 4, pp. 1461–1473, 2014. DOI: 10.1109/TCST.2013.2280464.

[34] W. He, S. S. Ge. Cooperative control of a nonuniform gantry crane with constrained tension. *Automatica*, vol. 66, pp. 146–154, 2016. DOI: 10.1016/j.automatica.2015.12.026.

[35] M. Yayla, A. T. Kutay. Adaptive control algorithm for linear systems with matched and unmatched uncertainties. In *Proceedings of the 55th Conference on Decision and Control*, Las Vegas, USA, pp. 2975–2980, 2016. DOI: 10.1109/CDC.2016.7798713.

[36] G. C. Yang, J. Y. Yao, G. G. Le, D. W. Ma. Asymptotic output tracking control of electro-hydraulic systems with unmatched disturbances. *IET Control Theory & Applications*, vol. 10, no. 18, pp. 2543–2551, 2016. DOI: 10.1049/iet-cta.2016.0702.

[37] H. B. Sun, L. Guo. Neural network-based DOBC for a class of nonlinear systems with unmatched disturbances. *IEEE Transactions on Neural Networks and Learning Systems*, vol. 28, no. 2, pp. 482–489, 2017. DOI: 10.1109/TNNLS.2015.2511450.

[38] B. Lu, Y. C. Fang, N. Sun, X. Y. Wang. Antiswing control of offshore boom cranes with ship roll disturbances. *IEEE Transactions on Control Systems Technology*, vol. 26, no. 2, pp. 740–747, 2018. DOI: 10.1109/TCST.2017.2679060.

[39] Y. Z. Qian, Y. C. Fang, B. Lu. Adaptive repetitive learning control for an offshore boom crane. *Automatica*, vol. 82, pp. 21–28, 2017. DOI: 10.1016/j.automatica.2017.04.003.

[40] W. He, S. S. Ge, B. V. E. How, Y. S. Choo, K. S. Hong. Robust adaptive boundary control of a flexible marine riser with vessel dynamics. *Automatica*, vol. 47, no. 4, pp. 722–732, 2011. DOI: 10.1016/j.automatica.2011.01.064.

[41] N. Sun, Y. C. Fang, H. Chen, Y. M. Wu, B. Lu. Nonlinear antiswing control of offshore cranes with unknown parameters and persistent ship-induced perturbations: Theoretical design and hardware experiments. *IEEE Transactions on Industrial Electronics*, vol. 65, no. 3, pp. 2629–2641, 2018. DOI: 10.1109/TIE.2017.2767523.

[42] N. Sun, Y. C. Fang, H. Chen, Y. M. Fu, B. Lu. Nonlinear stabilizing control for ship-mounted cranes with ship roll and heave movements: Design, analysis, and experiments. *IEEE Transactions on Systems, Man, and Cybernetics: Systems*, 2017, to be published. DOI: 10.1109/TSMC.2017.2700393.

[43] M. A. Hannan, W. Bai. Analysis of nonlinear dynamics of fully submerged payload hanging from offshore crane vessel. *Ocean Engineering*, vol. 128, pp. 132–146, 2016. DOI: 10.1016/j.oceaneng.2016.10.030.

[44] Q. H. Ngo, N. P. Nguyen, C. N. Nguyen, T. H. Tran, Q. P. Ha. Fuzzy sliding mode control of an offshore container crane. *Ocean Engineering*, vol. 140, pp. 125–134, 2017. DOI: 10.1016/j.oceaneng.2017.05.019.

[45] N. Sun, Y. C. Fang. New energy analytical results for the

regulation of underactuated overhead cranes: An end-effector motion-based approach. *IEEE Transactions on Industrial Electronics*, vol. 59, no. 12, pp. 4723–4734, 2012. DOI: 10.1109/TIE.2012.2183837.

[46] N. Sun, Y. C. Fang, H. Chen, B. Lu. Energy-based control of double pendulum cranes. In *Proceedings of IEEE International Conference on Cyber Technology in Automation, Control, and Intelligent Systems*, Shenyang, China, pp. 258–263, 2015. DOI: 10.1109/CYBER.2015.7287945.

[47] Y. Z. Qian, Y. C. Fang. Dynamics analysis of an offshore ship-mounted crane subject to sea wave disturbances. In *Proceedings of the 12th World Congress on Intelligent Control and Automation*, Guilin, China, pp. 1251–1256, 2016. DOI: 10.1109/WCICA.2016.7578629.

[48] N. Sun, Y. C. Fang, H. Chen. A new antiswing control method for underactuated cranes with unmodeled uncertainties: Theoretical design and hardware experiments. *IEEE Transactions on Industrial Electronics*, vol. 62, no. 1, pp. 453–465, 2015. DOI: 10.1109/TIE.2014.2327569.

Yu-Zhe Qian received the B. Sc. degree in automation from Nankai University, China in 2014. She is currently a Ph. D. degree candidate in control theory and control engineering at Institute of Robotics and Automatic Information System, Nankai University, China.

Her research interests include nonlinear control and control of underactuated mechatronic systems including offshore ship-mounted cranes.

E-mail: qianyzh@mail.nankai.edu.cn
ORCID iD: 0000-0002-9734-2132

Yong-Chun Fang received the B. Sc. degree in electrical engineering, and the M. Sc. degree in control theory and applications from Zhejiang University, China in 1996 and 1999, respectively, and the Ph. D. degree in electrical engineering from Clemson University, USA in 2002. From 2002 to 2003, he was a postdoctoral fellow with the Sibley School of Mechanical and Aerospace Engineering, Cornell University, USA. From 2011 to 2012, he was a visiting professor at Holcombe Department of Electrical and Computer Engineering, Clemson University, USA. He is currently a professor with Institute of Robotics and Automatic Information System, Nankai University, China. He is a senior member of IEEE.

His research interests include nonlinear control, visual servoing, and control of underactuated systems including overhead cranes.

E-mail: fangyc@nankai.edu.cn (Corresponding author)
ORCID iD: 0000-0002-3061-2708

Tong Yang received the B. Sc. degree in automation from Nankai University, China in 2017. She is currently a master student in control science and engineering, with Institute of Robotics and Automatic Information Systems, Nankai University, China.

Her research interests include the nonlinear control of underactuated systems including rotary cranes and offshore cranes.

E-mail: yangt@mail.nankai.edu.cn
ORCID iD: 0000-0002-5682-4223